IRP FInal Report: October 2014 to December 2017

DoE Project #14-7353 CID #DE-NE0008305

Advanced Instrumentation for Transient Reactor Testing

Principal Investigator
Michael L. Corradini
Professor, Engineering Physics
University of Wisconsin, Madison WI 53706
Corradini@engr.wisc.edu
Phone: (608) 263-1648

Co-Principal Investigators:
Mark Anderson, Professor, University of Wisconsin-Madison
George Imel, Professor, Idaho State University
Tom Blue, Professor, Ohio State University
Jeremy Roberts, Professor, Kansas State University
Kurt Davis, Scientist, Idaho National Laboratory

Project Period: October 2014 to December 2017

Reporting Period: October 2014 to December 2017

January 2018

INTEGRATED RESEARCH PROJECT SUMMARY

Transient testing involves placing fuel or material into the core of specialized materials test reactors that are capable of simulating a range of design basis accidents, including reactivity insertion accidents, that require the reactor produce short bursts of intense high-power neutron flux and gamma radiation. Testing fuel behavior in a prototypic neutron environment under high-power, accident-simulation conditions is a key step in licensing nuclear fuels for use in existing and future nuclear power plants. Transient testing of nuclear fuels is needed to develop and prove the safety basis for advanced reactors and fuels. In addition, modern fuel development and design increasingly relies on modeling and simulation efforts that must be informed and validated using specially designed material performance separate effects studies.

These studies will require experimental facilities that are able to support variable scale, highly instrumented tests providing data that have appropriate spatial and temporal resolution. Finally, there are efforts now underway to develop advanced light water reactor (LWR) fuels with enhanced performance and accident tolerance. These advanced reactor designs will also require new fuel types. These new fuels need to be tested in a controlled environment in order to learn how they respond to accident conditions. For these applications, transient reactor testing is needed to help design fuels with improved performance.

In order to maximize the value of transient testing, there is a need for in-situ transient real-time imaging technology (e.g., the neutron detection and imaging system like the hodoscope) to see fuel motion during rapid transient excursions with a higher degree of spatial and temporal resolution and accuracy. There also exists a need for new small, compact local sensors and instrumentation that are capable of collecting data during transients (e.g., local displacements, temperatures, thermal conductivity, neutron flux, etc.).

PROJECT OBJECTIVES

The ability to monitor fuel behavior in real-time is the focus of our Integrated Research Project. Our team effort is aimed at providing more information on the time evolution of the fuel rod state, which is important to develop a thorough understanding of the underlying science of fuel behavior. Such measurements could also provide real-time data that can substantially compliment sole reliance on post-irradiation examination (PIE), which only provides data on the final state of fuel rod components.

Our research team seeks to develop and demonstrate specific new and innovative measurement diagnostics for real-time in-situ monitoring to support transient reactor testing. Our objectives has three key program elements:

- Develop innovative concepts that lead to the design of the next generation fuel motion monitoring system to support transient testing, taking advantage of 'line-of-sight' core layouts; i.e., advancements in spatial and temporal resolution for hodoscope imaging.

- Develop novel instrumentation to support in-pile transient testing that includes fast response displacement and temperature measurements, thermal conductivity measurements, local fast and thermal neutron flux measurements.

- Demonstrate these novel instrumentation measurement methods in a reactor environment using university TRIGA reactors as well as design for their use in a transient test reactor.

As discussed within our original proposal, prior transient testing experience indicates that the sensors and methods identified for investigation within this project are important for obtaining most of the required key parameters and data from transient tests and for meeting data validation needs

This Advanced Instrumentation for Transient Reactor Testing IRP combines the expertise of four universities and a leading national laboratory (and its unique instrumentation laboratory and staff expertise) with an international partner that provides instrumentation and test rigs. The IRP research team functions as a matrixed engineering team that is focused on our five distinct task areas:

- Task I: Development of innovations for real-time, 'line-of-sight' imaging for a transient test using the current hodoscope concept with advancements in detection and image resolution;

- Task II: Development of novel sensors to measure local displacements and temperatures of fuel rod under transient conditions as well as local measurements of neutron fast and thermal flux;

- Task III: Out-of-pile testing of these novel sensors under a common test protocol and geometry;

- Task IV: In-pile testing of these instruments in a TRIGA reactor to demonstrate the capability to measure these key parameters in a radiation environment under transient conditions;

- Task V: Preliminary Design of Standard Transient Reactor Experiment Test Capsules with Advanced Instrumentation.

PROJECT ACCOMPLISHMENTS DURING THE PROJECT PERIOD

Task I: Hodoscope Technology Enhancements

Hodoscope and Collimator Support

Cloud Chamber

The feasibility study of a hodoscope using a cloud chamber without a collimator was performed. The optimum liquid combination of ethyl alcohol and water that give low expansion ratio, low background fog and good electron tracks in the chamber was found to be 67% of alcohol and 33% by volume of water. Using this composition, several runs were performed to get better trails. Unfortunately, the tracks were quite faint and lasted for very small fractions of seconds. Clearly, the disruptive movement of the gas was noticed. At this time we determined that using our cloud chamber would not be a viable option, even if it has several advantages. We turned our efforts to simulation of the image and de-convolution techniques.

MCNP Simulation

A detailed model of the TREAT reactor was built in MCNP with the central fuel element replaced by a slotted fuel element containing the sample. This provides an open path between test samples at the center of the core and hodoscope detector. In the MCNP output file, the point flux tallies and the mesh tally were added to determine the flux at different distances from the center to the hodoscope location. Flux data at varying distance were imported and plotted. The average and uncollided vertical flux profile at the hodoscope plane (x=hodoscope distance, y=0) was determined. The average flux profile was expanded using spherical harmonics to get the image coefficients, which were later used to get the object coefficients using analytical approach briefly described below.

Analytical Approach of Back Projection

After obtaining the flux plots, an approximate fit to the flux profile was performed to get a general function that describes the behavior. This arbitrary function was then expanded in spherical harmonics using the properties of orthogonality and completeness. Several expansion coefficients were calculated using Mathematica 9.0.1 (Wolfram Research Inc., 2013). After finding the coefficients, they were used back in the expansion to see if the coefficients build up to give the original profile. Both the plots look similar to what they were supposed to be and those coefficients built up to give the profile and this analytical method could be used to any general function (Note: this will be quantified in future work, which we are funding internally). Since the image is formed by the convolution of the object function (source profile) and the point spread function (PSF) of the imaging system, the PSF of the pinhole needs to be determined. In the analytical derivation of PSF, we assumed the far-field region also called the Fraunhofer region approximation in classical diffraction theory. In the far-field region, diffraction can be related using the Fraunhofer equation and the corresponding PSF follows a Gaussian distribution. PSF of the pinhole gives the degree of blurring caused by diffraction and this function is later used to extract the right beam size out of the pinhole image. Using the image coefficients and the PSF of the pinhole, source information will be ascertained analytically. Validation of this analytical model is yet to be done with any experimental data. We are pursuing this with internal resources,

and if successful will be able to determine the uncertainty and the accuracy of the model. This will be presented in the literature in the future.

Hornyak-button Alternatives

Three candidate technologies were modeled, constructed, and tested to varying degrees. These technologies included variants of microstructured neutron detectors (MSNDs) based on hydrogenous or actinide reactants; devices based on ZnS(Ag) that represent evolutions of the original Hornyak button; and a CF_4H_2-based, gas-scintillator detector.

Of these candidates, the two most promising technologies to emerge were (1) a paraffin-loaded MSND and (2) a device consisting of alternating layers of ZnS(Ag) and Lucite with silicon-photomultipliers (SiPMs) attached at the sides for light collection. Both devices were modeled using MCNP and Geant4 (as applicable). The hydrogenous MSND (h-MSND) was predicted to have an efficiency greater than 15% for mono-directional, fission-spectrum neutrons and a device length of 5 cm along the beam path. The layered ZnS(Ag) device was predicted to have an efficiency of approximately 3.5% for a 5 cm device. For comparison, the original Hornyak button was reported to exhibit efficiencies on the order of 0.1%. The efficiencies predicted were based on lower-level discriminator (LLD) settings sufficiently large to achieve signal-to-noise ratios of 100 for an assumed gamma-ray background consistent with the literature.

In-beam tests at the KSU reactor confirmed that the h-MSND can detect fast neutrons. However, future testing will require beam filters to knock down contributions from thermal neutrons and gamma rays. A layered ZnS(Ag) device was constructed and tested using a Cf-252 source. The measured efficiency compares well to predicted results and outperformed an existing Hornyak button acquired from Idaho National Laboratory.

Task IIA: Micro-Pocket Fission Detectors (MPFD)

Micro-pocket fission detectors (MPFDs) have been a focus or component of several ongoing, DOE-supported projects. Their small size and relative insensitivity makes them ideal for in-core, real-time monitoring at a variety of power levels. Although tests were (and continue to be) performed early in the project, the focus shifted mid-way through the project following discussions with others (including G. Imel at ISU). Because TREAT transients are so large, the resulting fluxes and, hence, fission rates can become large enough to deposit large amounts of energy in a small mass.

Experiments were performed in the KSU TRIGA reactor to understand how a reactor pulse affects an MPFD reactant. Images of several alumina disks with natural uranium deposits were taken before and after the reactor pulse. The results confirm that the surface morphology of the deposition does change and that study would be needed prior to deployment in TREAT.

Cross-calibration Measurements: ISU collaborated with KSU in support of the development of the Micro-Pocket Fission Detector. Specifically, ISU helped in the cross-calibration efforts, to reduce the uncertainties in the measured fission rates.

Initial neutron-induced fission event measurements were performed using an old back-to-back fission chamber (BTBFC) in a paraffin surrounded "cave" with a 3.5mCi Cf-252 source. The BTBFC was loaded with a U-235 standard foil (~120 μg U-235). The U-235 standard was made and well characterized by Argonne National Laboratory for the purpose of real-time neutron flux detection and cross-calibration measurements.
The results of the initial tests provided fission event pulse-height information for selecting the proper accompanying amplifying electronics and settings. However, given the extremely low count-rates ~0.5 counts/min, no further measurements were made, and the setup was then moved to the AGN-201 test reactor's thermal access port.

Testing in the AGN-201 first revealed noise issues related to connection problems occurring with the old BTBFC used in the initial paraffin tests. The BTBFC was swapped with the "legacy" BTBFC. The "legacy" BTBFC was made by Argonne National Laboratory compared to the previous BTBFC which was made at Idaho State University. The change to the "legacy" BTBFC—referred to as the OD 1.4 in. BTBFC—also required a change in preamplifier to match the larger capacitance of the detector. Additionally, an attenuator was built and connected before the amplifier to prevent pulse clipping from the amplifier. Results from cross-calibrating between the U-235 standard and the KSU sample, NFT.U.250.5, revealed issues of burnup in the U-235 standard due to the extremely low count-rate of the KSU samples (That is, we would have to count too long to get adequate statistics thereby burning the standard out rapidly.). Results from cross-calibrating between two KSU samples, NFT.U.250.5 and NFT.U.250.6, indicated a significant background affecting cross-calibration calculations with KSU samples. The background was determined to be associated with contamination of the fission chamber equivalent to approximately 0.5 μg of natural uranium; similar in mass to the KSU samples. Additionally, the count-rates with KSU samples inserted were still too low for significant counting statistics. To eliminate background associated with contamination and to increase the count-rate, a smaller BTBFC was built.

The new OD 0.8125 in. BTBFC was designed for cross-calibration measurements between KSU samples. The smaller diameter of the detector allowed access to the core center of the AGN-201 test reactor instead of the shielding region of the thermal access port. Accessing the core center of the reactor increased the count-rates by an order of magnitude—a satisfactory level for achieving proper counting statistics within reasonable operation time. The operating voltage from the power supply was determined to be 300V. Holders for the BTBFC was made to study the effects of detector position and orientation and ensure repeatability in detector setup. Following measurements with the holder were taken to further confirm repeatability in data collection.

The U-235 standard can only be used in the OD 1.4 in. BTBFC and cannot be directly used to cross-calibrate with KSU samples due to burnup. Gold foil was used as an intermediary to relate the U-235 fission rate results measured in the OD 1.4 in. BTBFC to the fission rate

results of KSU samples measured in the OD 0.8125 in. BTBFC. By loading half of the BTBFC with a small piece of gold foil and the other half with the U-235 standard or KSU sample, it is possible to relate the fission rate of separate measurements by gold foil activation analysis.

Using the gold foil activation analysis to properly scale the integrated flux experienced by the fissile deposits, the mass of KSU deposits were calculated in relation to the U-235 standard. The calculated masses were found to have same magnitude as reported by KSU's alpha-particle spectroscopy. However, the masses of all three samples were nominally lower than the initial reported mass ranges. The samples have since been returned to KSU for a final alpha-particle spectroscopy measurement to adjust the original report if needed. We are also hoping for some destructive wet chemistry to ultimately obtain the mass of the samples. We are continuing this work with the support of INL.

Related Work

Several smaller efforts have been undertaken in support of the two primary goals. First, a senior design team was tasked with producing a mock-up hodoscope for installation perpendicular to a the penetrating beam port of the KSU reactor. The team based their design on the existing hodoscope at TREAT, and had existing steel plates milled with 4 mm square channels bolted together to provide a 25-channel collimator. Ultimately, the team made some poor assumptions and were unable to develop an in-beam target to provide a sufficient, fast-neutron source for testing. However, the collimator remains in place for follow-on testing should such an appropriate source be acquired.

A related effort was made to model and analyze the penetrating beam port. This beam's spectrum is harder than the other beams but is still highly thermal. The KSU reactor model was extended to include the full extent of this beam. Advanced variance reduction techniques were applied to produce estimates of the beam spectrum, which are now being used to design an appropriate filter for in-beam, detector tests. Some in-beam spectroscopy has been performed using a set of Bonner spheres. It is expected this work will continue as part of ongoing efforts to improve estimates of various characteristics.

Task IIB: Diamond Diode Temperature Sensor

In this task, we have successfully fabricated a working diamond thermistor device inside a stainless sheath tube. The operation range of the thermistor device was from 350 ^{0}C to 920 ^{0}C. This has led to a patent disclosure as well as a journal article submission. This maximum temperature was mainly limited by the silver paste, which was used to attach Nb wires to the metal pad of the diamond. The melting point of the paste is 960 ^{0}C at the pressure of atmospheric pressure, and the silver paste used for our devices shows failure of electrical conduction above 920 ^{0}C.

Work is still continuing to extend the thermistor operation closer to the theoretical limit of the diamond thermistor to near 2000^{0}C. This work is continuing with collaboration of the HTTL team at INL under a separate LDRD effort. To extend the maximum temperature of the diamond thermistor, we replaced silver paste with laser welding process to attach

electric wire to the metal pad. Laser welding process is a welding process using a focused laser pulse at a welding spot. The diameter of the laser spot size is 100 μm and the laser pulse time is few msec, which makes the welding occurs instantly on the targeted spot. However, an intermediate material is need between the metal wire and the diamond metal pad since the thickness of the diamond metal pad is only 300 nm. To protect the diamond from the laser pulse, we chose Ni for the intermediate material. The melting point of the Ni is 1455 ^{0}C, which is expected to increase the maximum temperature of the diamond thermistor operation. To deposit thick Ni pad on top of the diamond metal pads, we planned to use electrolytic Ni plating process and simulated the optimum thickness of the Ni layer required for the laser welding process. The laser parameter is 0.39 J for the laser energy, 4 msec of laser pulse time which results 97.5W at the 100 μm diameter of the laser spot. The maximum temperature is over 9000 ^{0}C at the center of the spot. We further changed Ni layer thickness to simulate the temperature at the interface between the diamond and the Ni pad. The interface temperature shows temperatures of 96 , 127 , 172 , 250 , 415 , 575 ^{0}C respectively for Ni pad thicknesses of 250 μm, 200 μm, 150 μm, 100 μm, 50 μm, and 25 μm, respectively. As the thickness of the Ni layer increases, the temperature at the interface showed less, which has less chance to damage the diamond. During the Ni plating process to deposit thick Ni pad, we realized Ni pad only deposits on the backside of the diamond, which had rough surfaces. The front side of the diamond has smooth surface, which decreased the adhesion of metal pad to the diamond. We intentionally roughened the front side of the diamond to make rough surface to increase the bonding area to improve the adhesion. We have measured the roughness of the diamond surface with 3D optical surface profiler to ensure the surface is rough enough for the Ni plating process. The average surface roughness was 1 nm before grinding process and the average roughness increased to 240 nm after grinding. With roughened diamond samples, Ni pads were deposited on both sides of the diamond for the laser welding process to weld electrical wires.

For our future work on this thermistor development, we will collaborate with the HTTL research team. Using the INL's fabrication process, we will characterize the diamond thermistor operations at high temperature ranges. Another promising method to replace silver paste is using diffusion bonding process, which can replace laser welding method as well. We are under preparing stage for the diffusion bonding process experiments.

Task IIC: Fiber Optic Temperature Sensors

Fiber-optic sensors are being developed by both Ohio State (OSU) and Wisconsin (UW). The technology lead was Ohio State and Wisconsin implemented the Fiber Optic Sensors in out-of-pile and in-pile test vehicles for comparison testing and conducted integral experiments (see Task III and IV summary below).

Ohio State researched the feasibility of using fiber optics as a means of temperature sensing in reactor transient environments. Ohio State investigated two different types of optical fiber, silica glass fibers (SiO_2) and sapphire single crystal fibers (Al_2O_3), for use in TREAT for this IRP project.

Silica Optical Fibers

For silica glass optical fibers, OSU first tested commercial silica optical fibers (Corning SMF-28) to high temperatures to determine the temperature limit of distributed sensing in the fiber. Experiments revealed that the commercial fiber had a distributed temperature sensing limit of around 700 C. Above the 700 C mark, various effects such as annealing of the glass, atmospheric effects, and devitrification started to cause sensing failure in the fiber. By heat treating the fiber, the temperature range for distributed temperature measurements in commercial optical fiber could be extended to 800 C for continuous use and 900 C for short periods of time. Various microscopy techniques and numerous experiments determined that the silica fiber was most affected by the atmosphere surrounding the fiber at high temperatures. By placing the silica fiber in an inert or vacuum environment and having the fiber supported with a micro capillary tube or a high temperature coating, the distributed temperature measurement range of commercial silica optical fiber can be extended to 950 C.

For implementation into the TREAT reactor, research was done on ruggedizing the silica optical fibers. Metal coated fibers were experimented with, but unfortunately exhibited structural failure at temperatures around 900 C, due to the thermal mismatch between the metal and the fiber. Stainless steel capillary tubes were also investigated as a method for ruggedizing the fiber, but the stainless steel oxidized at 800 C causing the fiber to fail. Using a double tube setup, in which a silica micro capillary tube was placed in between the fiber and the stainless steel capillary tube, enabled the fiber to produce distributed temperature measurements up to 950 C. The silica micro capillary tube had a tight enough tolerance with the fiber that airflow to the fiber was sufficiently reduced creating an effective 'inert/vacuum' atmosphere around the fiber. The 'inert' atmosphere, combined with the extra strength of the tube, enabled measurements to be made with commercial fiber to 950 C, while also ruggedizing the fiber.

Silica optical fibers were also tested in a reactor environment (the Ohio State Research Reactor) to determine the radiation hardness of the optical fibers. It was found that distributed temperature sensing fails in commercial optical fibers in a nuclear reactor environment after a neutron fluence of around 10^{18} n/cm^2. OSU discovered that radiation hardness can be added to the distributed sensing ability of the fibers by inscribing Bragg gratings into them. Type-I Bragg gratings were shown to survive and produce temperature measurements for the entire duration of the reactor experiments conducted in the Ohio State Research Reactor, which resulted in a neutron fluence of around $2x10^{18}$ n/cm^2 and a gamma dose of 2 GRad. Type-II Bragg gratings have the most potential for long term use in a nuclear reactor, since they were shown to survive long periods of high temperature and high radiation fluence without degradation.

In Q11, OSU was invited up to the University of Wisconsin to participate in a heated reactor transient experiment to test the optical fibers ability to survive in a TREAT like environment. This experiment was designed to imitate the temperatures and radiation fluence that the fibers would experience in a TREAT experiment. To achieve the environment of this scenario, the Wisconsin TRIGA Reactor was ramped quickly to 1 MW,

while simultaneously heating the fibers in an enclosed test vehicle. The test vehicle was a watertight housing that was backfilled with Helium and contained a SiC heater to simulate the high temperatures that would normally be seen in a TREAT test. The test vehicle was lowered into a basket in the core grid on the periphery of the core. Once the test vehicle was secure in the core basket, the heater was turned up to 400 C inside of the test vehicle. Shortly after reaching a steady state temperature of 400 C, the reactor was quickly ramped to 1 MW. After 10 minutes, the reactor power was dropped back to 300 watts and this process was repeated at increasing temperature increments of 100 C until a 1000 C temperature was reached.

Two different types of optical fiber were used in this experiment, Corning SMF-28 fiber and Type-I Bragg grating optical fiber with gratings every 1 cm. The temperature measurements of the SMF-28 fiber seem to follow the temperature of the furnace very accurately until the reactor power was ramped up. During reactor irradiation, the fiber had null measurements about every other measurement, which resulted in a measurement of zero for the temperature. Once the reactor was turned back off, the measurements of the fiber continued without the null measurements. This phenomenon occurred at each temperature step over the duration of the experiment until the temperature of the vessel hit 900 C at which point, the fiber failed completely. The Bragg Grating fiber, performed much better during reactor irradiation compared to that of the SMF-28 fiber. The Bragg grating fiber did not produce the null measurements that the SMF-28 fiber produced during reactor irradiation, and was able to maintain a constant temperature measurement until the fiber temperature hit 800 C. At 800 C, the Bragg gratings partially annealed out in the fiber, causing the fiber to produce null measurements during reactor irradiation. The Bragg grating fiber was able to measure temperatures up to 900 C, before finally failing after the second to last reactor transient. The optical fiber and thermocouple measurements showed great correlation (within 5 C) until the temperature reached 900 C (at 900 C the fiber measurements failed). The high accuracy of the optical fiber with the thermocouple indicates that the use of optical fibers for temperature instrumentation in transient reactor environments is plausible.

When the reactor was ramped up to full power, the SMF-28 experienced difficulties in measuring the temperature. We conclude that this was due to the neutron and gamma flux of the reactor, since the temperature measurements stabilized once the reactor was turned off. The combination of high temperature and irradiation must have caused the measurement signal to skew as we have never seen this behavior before when conducting room temperature reactor experiments. The Bragg grating fiber was able to provide a constant measurement, even during reactor irradiation, due to the high signal to noise ratio of the reflections off of the Bragg gratings in the fiber. The Bragg gratings eventually degraded and annealed at temperatures of 800 C and so future experiments should investigate Type-II Bragg grating fiber. Type-II Bragg gratings have shown thermal stability up to 1000 C and would thus provide the temperature range along with the constant signal during reactor irradiation.

In conclusion, for silica glass fibers, OSU found that normal SMF-28 fiber has a temperature limit of around 900 C and a radiation fluence of around $8x10^{17}$ n/cm^2. For silica fiber with

inscribed Type-II Bragg gratings, the temperature limits are around 1000 C and we have not found a radiation fluence high enough (>$2x10^{18}$ n/cm^2) to disrupt sensing in the fiber. When combining temperature and radiation, SMF-28 fiber provides null data when the reactor is at high power, while Bragg grating fiber provides a steady measurement signal. In conjunction with the testing, we have also found ways to ruggedize and package the fiber sensor for instrumentation into the TREAT reactor.

Sapphire Optical Fiber

For sapphire fibers, we have made significant progress in making the sapphire fiber able to produce temperature measurements. Using sapphire fiber for sensing has been nearly impossible due to the multimodal nature of the fiber. The highly multimodal nature of sapphire is due to the large core size of the fiber and the lack of a reflective cladding in the fiber. OSU has invented a way to create a reflective cladding in sapphire fiber, while also reducing the core size of the fiber. This new cladding technique reduced the light modes in the fiber, enabling the sapphire optical fiber to produce distributed temperature measurements. This new sapphire fiber was tested to high temperatures (1000 C) and in radiation environments and showed zero degradation in either.

OSU developed a method of creating a near single mode sapphire optical fiber which enabled the sapphire optical fiber to produce distributed temperature measurements using the OFDR sensing technique. With a single mode sapphire fiber created, OSU inscribed Bragg gratings every 6 cm along the entire fiber to act as high temperature sensors. These sapphire sensors were tested under the following environments: during heating in the absence of radiation up to 1000 °C, during Co-60 gamma irradiation at room temperature and finally during reactor irradiation at room temperature.

The sapphire Bragg grating sensors were ramped to 1000 °C, in 100 °C steps, in a tube furnace. The sapphire Bragg gratings were able to produce stable and accurate temperature measurements at every temperature tested. The gratings showed zero degradation in regards to their reflected backscatter amplitude to temperatures up to 1000 C. The sapphire Bragg grating sensors have great potential for producing accurate temperature measurements at temperatures higher than a 1000 C, unfortunately, time restrictions caused a reduction in the scope of our testing. Tests to higher temperatures of the sapphire Bragg gratings is recommended for future work.

Following the high temperature tests, the cladded sapphire fiber with inscribed femtosecond Bragg gratings was tested for its radiation survivability. The radiation survivability tests consisted of two tests: a gamma ray only irradiation and a reactor irradiation (neutrons and gamma rays). The Ohio State Reactor Lab was used for both of these tests as the facility contains a 450 kW research reactor and a Co-60 irradiator. The sapphire fiber sensors were placed into the Co-60 irradiator and irradiated for a total of 5 full days. The gamma dose of the irradiator is approximately 23.1 kRad per hour. Over the 5 days of irradiation, the sapphire sensors accumulated approximately 2.82 MRads. The sapphire Bragg gratings were unaffected by the gamma rays as their reflective amplitude

never changed over the course of the experiment and the gratings produced a constant temperature measurement.

Following the irradiations in the gamma irradiator, the sapphire fiber sensors were transferred into the Central Irradiation Facility (CIF) dry tube located in the Ohio State Research Reactor. The CIF tube is an open air dry tube that is situated in the middle of the OSURR core. This experiment occurred during the OSU Reactor Lab's busy season and so unfortunately, we had reduced hours for 3 of the 4 days of irradiation. Nonetheless, the sapphire Bragg gratings appeared to have survived the irradiations in the OSURR and produced reasonable temperature measurements. The sapphire Bragg gratings were able to survive 1 GRad of gamma dose and a neutron fluence of 10^{18} n/cm^2 without showing degradation of the gratings. The survivability testing of the sapphire sensors was successful but the accuracy and precision of these sensors is recommended for future work.

Task IID, E, F: Fabricate and characterize HTTL Sensors for testing in rod geometry

The INL HTTL lab team fabricated and characterized the HTIR temperature measurement sensors (four devices specifically) and sent them to the UW for testing in the out-of-pile capsule as planned and has delivered the thermal conductivity probe and ultrasonic temperature (UT) sensor this year for out-of-pile and in-pile testing. All these instruments are described below.

In an effort to develop advanced fuels for LWRs as well as technology development for advanced reactors, transient testing is needed to develop and demonstrate the safety basis of these advanced systems. Compact sensors capable of collecting data during transient testing (e.g., temperatures, thermal conductivity, etc.) were developed in this project. Specifically, the High Temperature Test Laboratory (HTTL), located at Idaho National Laboratory (INL), developed and provided three specific instruments for use during this project. The three instruments provided were thermocouples, thermal conductivity probes and ultrasonic temperature probes. The development and construction of each instrument is discussed below.

Four high-temperature irradiation-resistant thermocouples (HTIR-TCs) were provided to support in-pile testing conducted in the University of Wisconsin reactor. The design and fabrication of HTIR-TCs was completed at INL as shown in Figure 1.

The design incorporated features to accommodate test conditions and geometry for the in-pile testing. Specifically, INL equipment was configured to fabricate HTIR-TCs for use in the expected temperature gradient. The primary temperature gradient for the TC decreases from 1500 °C to ~100 °C in an 18 inch length extending from the TC tip. Hafnia (HfO_2) insulation was used in this 18inch region. The remainder of the metallic sheath was insulated using alumina [Al_2O_3]. Heat treatment was achieved using a large horizontal tube furnace. During heat treatment the TC tip was heated to 1650 °C. Calibration to 1550 °C was completed in the same tube furnace using a NIST-traceable Type S TC as the reference. Unique geometry limitations required an innovative solution to ensure water-tight integrity of the HTIR-TCs. A minimum metallic sheath length of 22 ft. was originally specified to extend from the tip of the TC to an acceptable position above the reactor tank

water level. However, a single metallic sheath of sufficient length was not available and the pool-to-test pass-through could not accommodate a splice sleeve. For those reasons, a decision was made to fabricate the TC using a metallic sheath for the first 12 ft. A potting cup was then designed to transition from the metallic sheath to soft extension cable – below the water level. To ensure water-tight integrity, the potting cup also included barbs for attaching a Tygon PVC tube to the soft extension end of the cup without requiring a clamp. The Tygon tube, which contains the soft extension cable, extends well above the water level. (See Figure 1.) (Note that the water-tight integrity of the potting cup with Tygon tube was verified in a hydrostatic test over a period exceeding 2 weeks.)

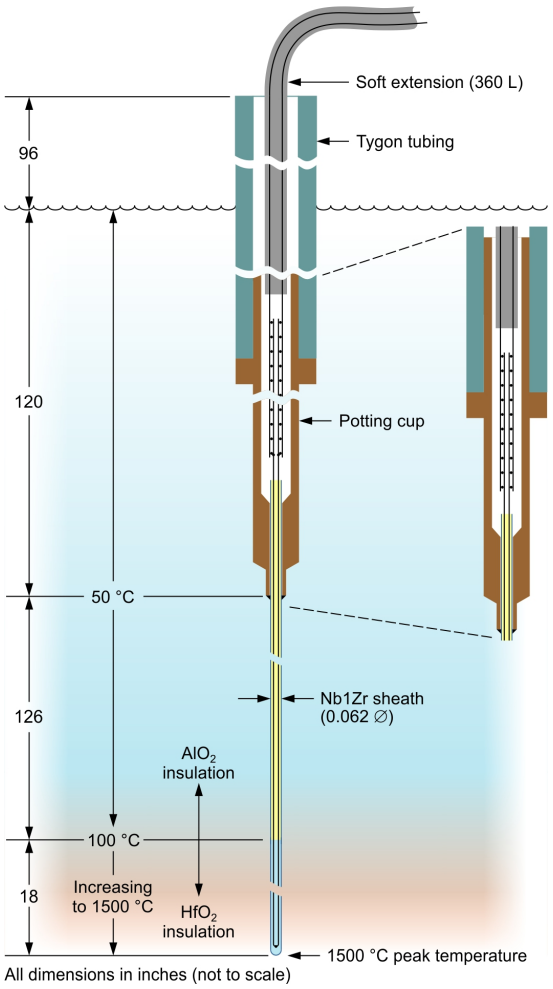

Figure 1. HTIR-TC design.

Pre-irradiation testing conducted at the UW-M exposed calibration and construction process weakness in the HTIR-TC. Temperature errors in excess of 2% were found and it was suspected that oxygen concentration levels of 1 ppm during the heat treat and calibration processes may have contributed to this error. The TCs were sent back to INL for re-heat treat and calibration. Changes were made to the calibration and heat treatment process that drastically reduced oxygen concentration levels ($1x10^{-15}$ ppm). Figure 2 shows

two niobium tubes that were subjected to heat treatment processes. The top tube was heat treated using the old process while to bottom was heat treated using the new process. After heat treatment each tube was subjected to a bending test. The top tube failed with a brittle fracture while the bottom tube was found to maintain its ductility. A pronounced benefit of this change is that HTIR-TC can now be manufactured to be ductile. This greatly enhances installation of future HTIR-TCs, making it possible to install it in test trains that require bending of the thermocouple.

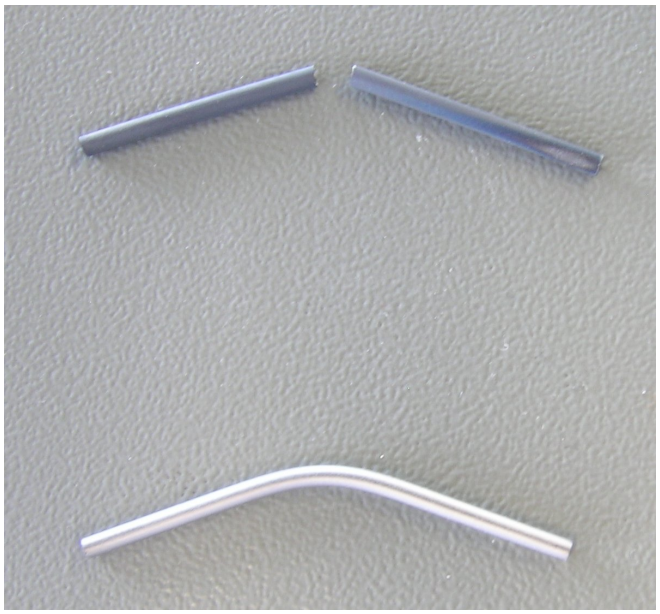

Figure 2. Bending of Niobium sheath (top) subjected to heat treatment process at (1 ppm O_2) and Niobium sheath (bottom) subjected to improved heat treatment process.

Two transient hot wire method (THWM) thermal conductivity probes were also constructed at INL (See Figures 3 and 4). The probes are capable of measuring thermal conductivity up to 1100 °C. The 1100 °C rating is based on the use of a type K thermocouple in the heated section of the probe. The first 100 mm of the extension section is capable of withstanding temperatures up to 800°C. This limit was established through performance testing of the heater extension wire weld. Nondestructive evaluations of the welds were also performed using 3D computed tomography.

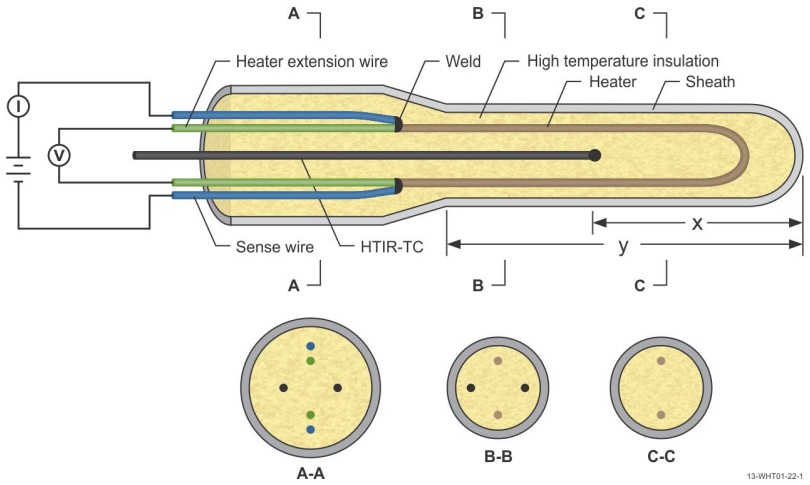

Figure 3. Schematic of the THWM thermal conductivity probe.

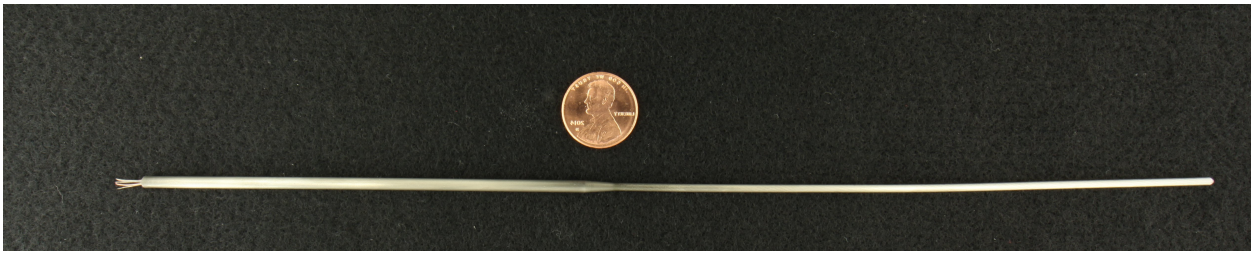

Figure 4. Photo of Prototype 1 with penny for optical scale.

In addition to the weld evaluations, 3D computed tomography was used to evaluate other portions of the probes. Figure 5 shows a cut away image of prototype probe 3 for the area between A-A and B-B shown in Figure 1. Computed tomography found contact between the sense wire and the heater extension in all of the probes scanned, see Figure 6. The length of contact can be as much as 30 mm. This contact region can affect the power distribution in the probe. To accommodate for the contact, a correction factor was applied to the mathematical model.

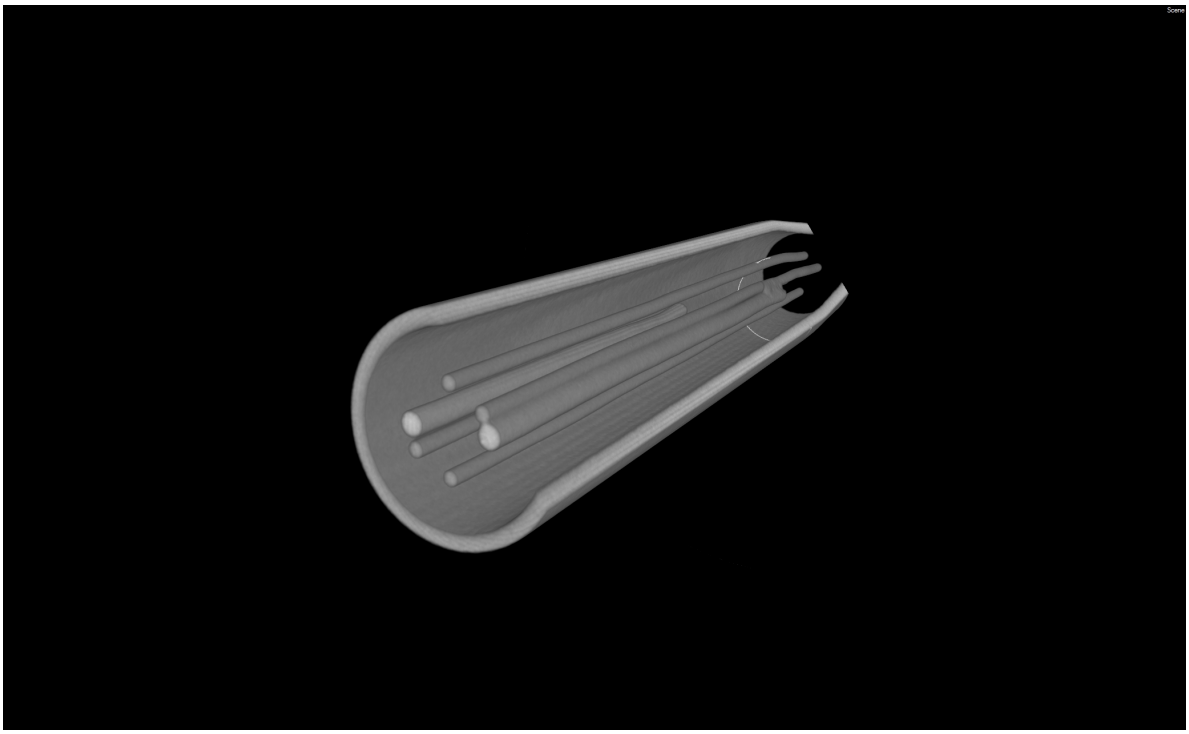

Figure 5. Computed tomography scan of prototype probe 3.

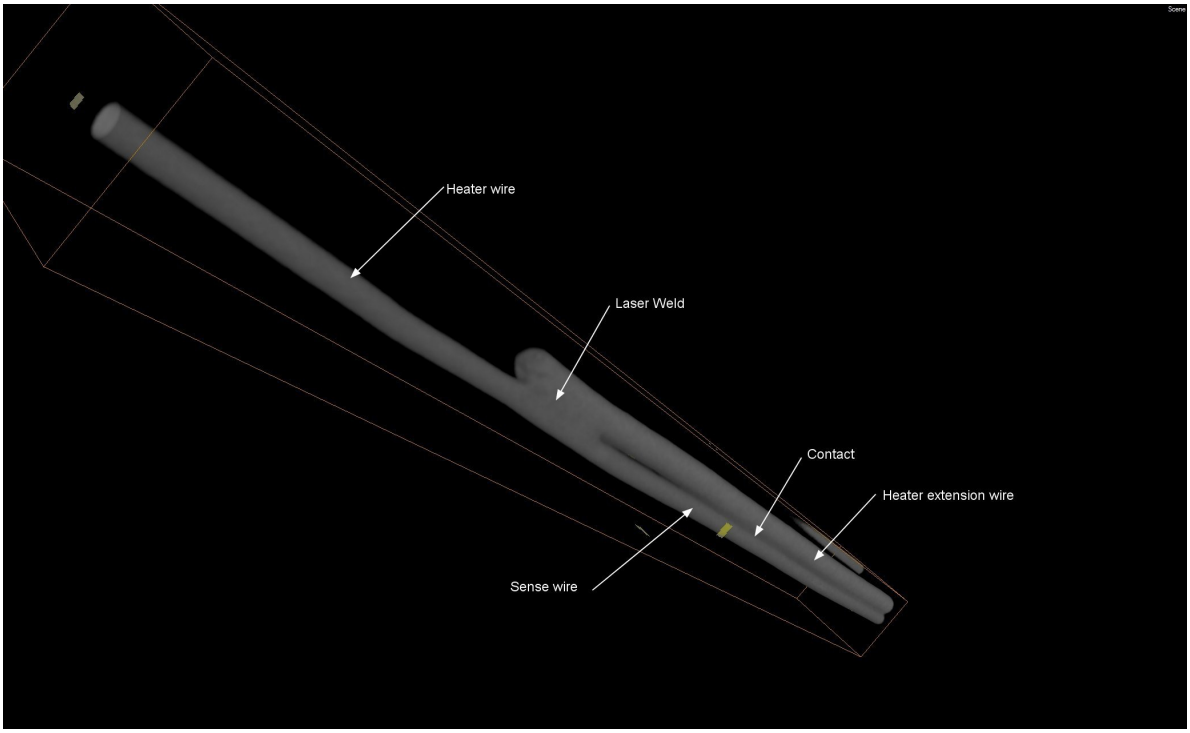

Figure 6. Computed tomography scan of prototype probe 3 showing the contact between the sense wire and the heater extension wire.

Prototype probe 3 was tested in fused silica at 20°C and 250°C. Figure 7 shows Probe 3 inserted in the fused silica (b) which was then inserted in the furnace (a). Figure 8 is a plot of the thermal response of Probe 3. An input power of 4 W with an initial steady state temperature of ~240°C was used. Using the mathematical model with the correction factor and the data from this test, the calculated thermal conductivity showed good agreement (< 8% error) with published data.

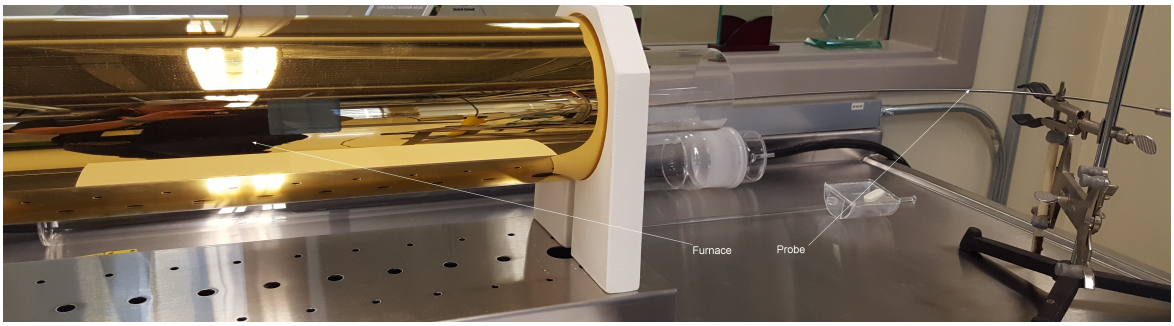

(a)

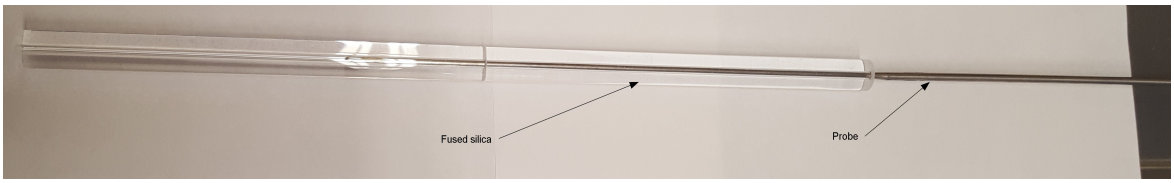

(b)

Figure 7. Performance testing of the probe at 250°C.

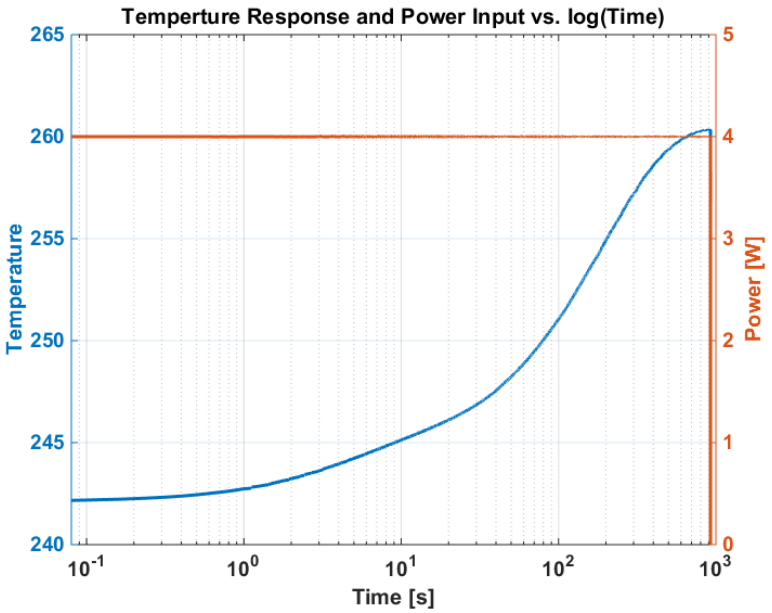

Figure 5. Thermal response of prototype probe 3 in fused silica with an initial steady state temperature of ~240°C.

As part of this project, a new control and analysis software package provided by the French Atomic Energy Commission (CEA) was implemented. Figure 8 shows a screen capture of the analysis interface. This new software provided enhanced power control and a time saving user interface. Construction and testing of the THWM thermal conductivity probe was completed at INL and delivered to the UW-M. Training on the system was also provided. Figure 9 shows the components delivered to the UW and is still being tested.

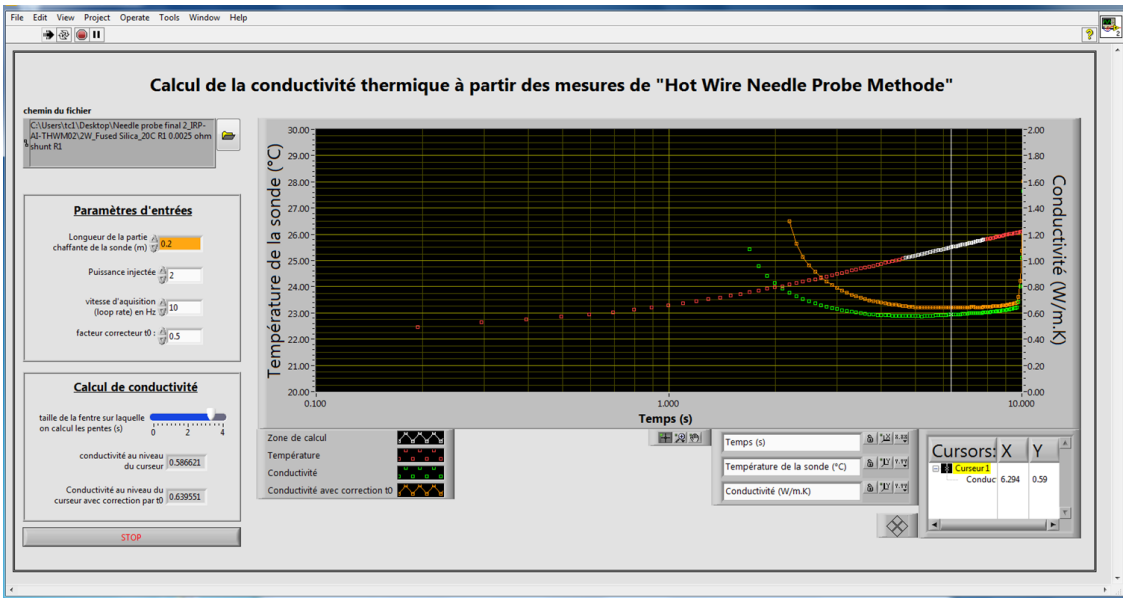

Figure 8. Screen shot of the test using CEA software with fused silica at 20°C.

Figure 9. Thermal conductivity probe components delivered to UW-M.

Three ultrasonic thermometers (UTs) were constructed at Idaho National Laboratory (INL) and delivered to UW-M along with a pulser/receiver system. Training was also provided. A schematic of a typical UT is provided in Figure 10.

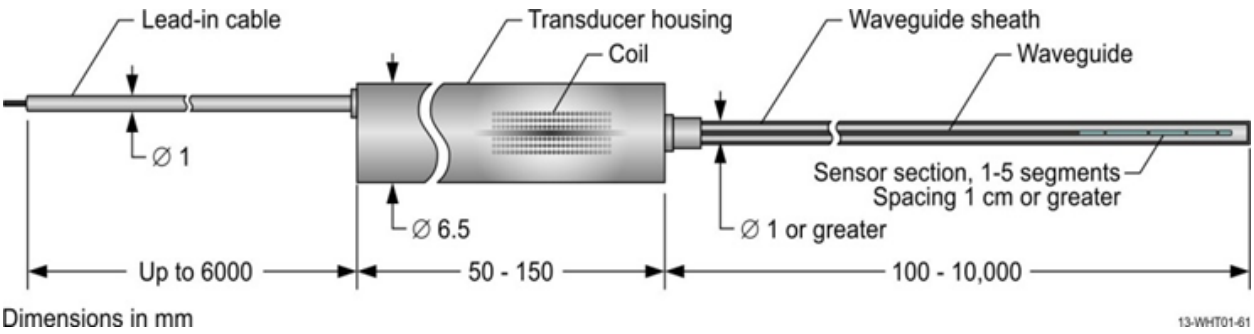

Figure 10. Typical representation of an ultrasonic thermometer.

The UT construction process is relatively complicated. Figure 11 shows a UT at several steps in the fabrication process.

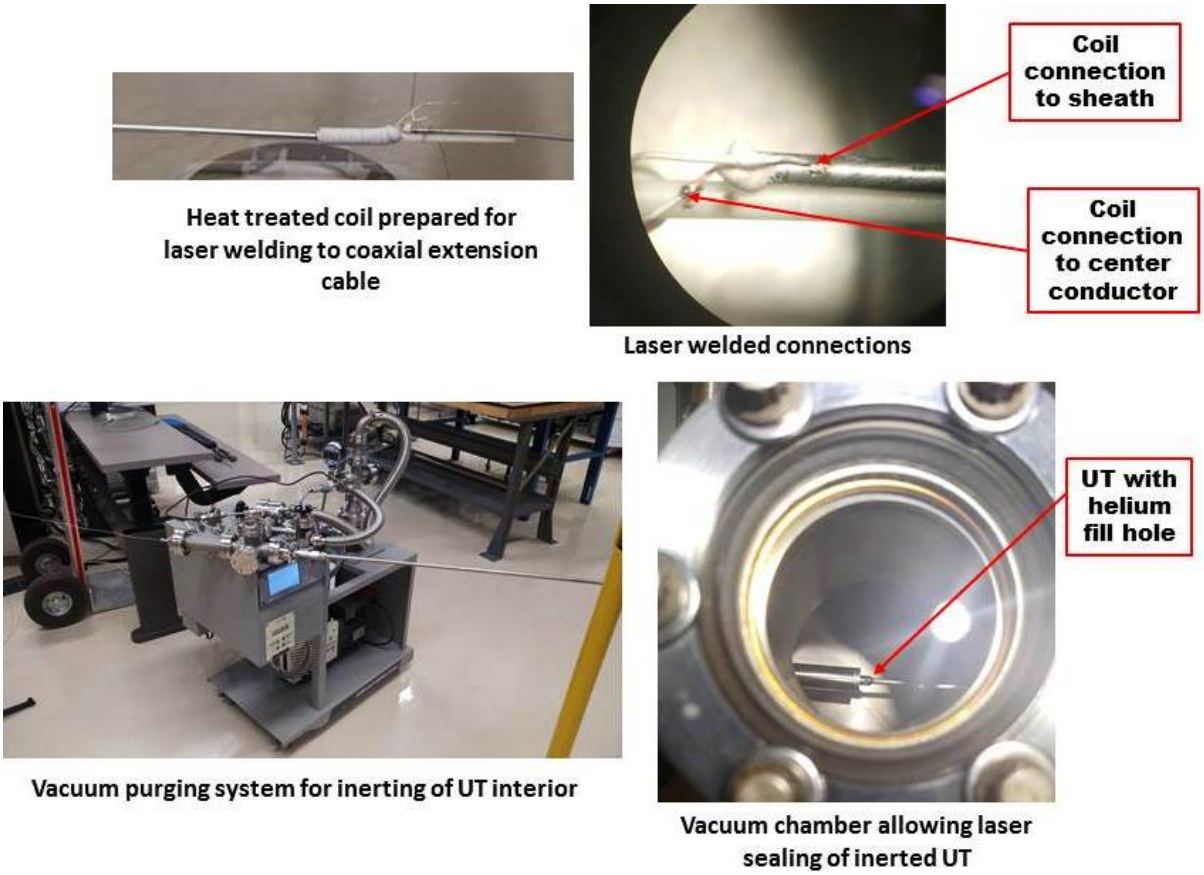

Figure 11. Fabrication steps and electronic equipment for Ultrasonic Thermometer.

Three different UTs were constructed. The UTs delivered are identified as Molybdenum, Inconel and Inconel Multi-Segment. The Inconel Multi-Segment contained 4 temperature sensing segments while the other two contained only one. During the calibration process, the maximum temperature was established due to signal attenuation. Table 1 gives sensor temperature limits. Figure 12 presents the normalized calibration data for each sensor. The calibration data was found to be acceptable, with the exception of the Inconel Multi-Segment 3. Poor calibration was the result of low signal amplitude caused by a manufacturing flaw. UW successfully tested these in out-of-pile and in-pile experiments.

Table 1. Sensor temperature limits established during calibration.

Sensor	Configuration	Maximum Temperature
Molybdenum	Single temperature sensor	1500 °C
Inconel	Single temperature sensor	900 °C
Inconel Multi-Segment	Four temperature sensors	900 °C

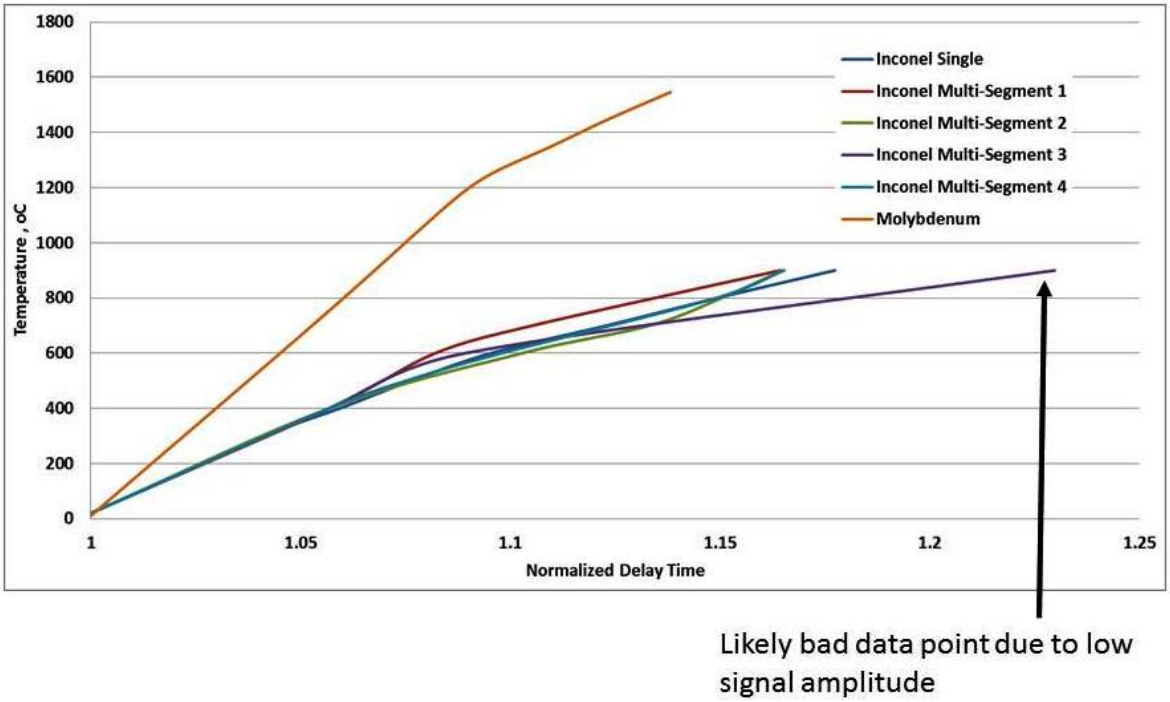

Figure 12. Normalized calibration data for the UTs.

Summary:

Four HTIR-TCs, two THWM thermal conductivity probes and three UTs were provided to support in-pile testing conducted in the University of Wisconsin reactor. A pronounced

benefit of this project is that HTIR-TCs can now be manufactured to be ductile. This greatly enhances installation and future use of HTIR-TCs, making it possible to install them in test trains that require bending of the thermocouple. Another benefit resulting from this project is the new control and analysis software package provided by CEA for the THWM thermal conductivity probe. This new software provides enhanced power control and a time saving user interface. Finally, this project provided advancements in the development of UT sensors with new material choices capable of measuring temperatures to 1500°C.

Task III and IV:

Both out-of-pile and in-pile experiments were completed. A detailed report of this work has been uploaded to our PICS website. This work provides a demonstration by experiment and supporting analysis of the capacity of several advanced temperature sensor to make local temperature measurements during transients in a radiation environments, as would be found in a light water nuclear reactor environment. This work has also quantitatively characterized several specifications of the sensors, such as precision and accuracy of temperature measurements, measurement of the time response for the sensor, effect of the fiber sheath used on the sensor, and the minimum neutron fluence values for sustained sensor functionality.

The testing of the array of sensors is complimented with the in-depth investigations into the chief causes of limitation and failure of the fiber optic sensor and subsequent improvements to the sensor design. The currently available set of local temperature sensing instrumentation brings with it limitations that are a major hindrance to the development and potential of advanced reactor designs. From the inability of high temperature RTDs to be deployed in a high radiation environment to the poor temperature maxima of 1200°C for radiation hard thermocouples to the cripplingly low spatial resolution of both types, advanced sensors are a much needed development to support the growth and progress to be made in many other areas of the nuclear industry.

The fiber optic distributed temperature sensor has proven resilient in radiation environments, functioning with standard deviations under 3°C regardless of radiation flux size or total fluence received. Though suffering from a slightly lower precision compared to other temperature sensors, the fiber sensor offers the incredibly high spatial resolution of a 0.64 mm sensor spacing and total sensing lengths in excess of tens of meters. This thesis has demonstrated the value of various aspects of fabrication concerning the fiber sensors (heat treatments, steel sheaths, inert gaseous environments, etc.) as well as suggestions for the better methods to employ when implementing them. This work presents the data to support the theory that hydrogen is the main chemical agent responsible for degradation of the fiber's ability to transmit light both at high temperatures and in radiation environments. It also shows the efficacious nature of the solutions provided to combat this mode of sensor failure. By incorporating the inert sheath and removing the fiber coating, hydrogen-caused attenuation of the fiber signal is limited to less than 2 dB/m for all combined high temperature and radiation induced effects. Measurement of the temporal impact the sheath and cover gas has on the sensor is measured to be 0.237 seconds and the positive proof of the fiber sensor's ability to function inside of a nuclear research reactor

without signs of deterioration is definitively displayed at temperatures up to 900°C.

The sensors from our INL HTTL team showed promising results. The HTIR-TC performed well both in and out of radiation environments showing no observable drift, impairment of precision, or signal loss as a result of irradiation. It always maintained a margin of error below 2% though was found to be highly sensitive to even the slightest traces of oxygen (showing severe signal drift for O_2 levels as low as 1ppm). The HTIR- TC also has a calibration issue, which may result in an offset in the accuracy of its readings stemming from an unidentified cause. The UT sensors did not perform as well in that the only one of the three sensors which functioned properly had standard deviations from ±14.3°C at temperatures above 400°C but dropping to ±35.56°C for the broader 0-850°C range. The total failure of the high temperature molybdenum sensor as a result of internal mechanical interference from fabrication error makes clear the need to improve upon the process of insulating the waveguide wire. Similarly, the lack of a proper transformation equation for the otherwise seemingly functional multi-segment Inconel sensor indicates an additional need for standardization of the calibration process and improvement in data acquisition software. Nevertheless, the single-segment Inconel UT did show its capacity to accurately measure local temperatures through a temperature transient up to 850°C.

All of these sensors have had their theoretical temperature sensing capabilities validated so that the next steps to be taken are as imminent as they are important. Opportunities for improving our understanding of the fiber sensors particularly include an advanced study of the impact that the termination has on the fiber sensor and then how to optimize the addition of that component. Another topic regarding the future work of the fibers is the impact that keying the fibers at an elevated temperature may have on the measurable temperature range. Both of these are topics about which little is well documented but which may have a substantial influence on the functionality of the fibers.

Regarding the HTIR-TC, further investigation is needed into the cause(s) of the offset sometimes observed in the sensors. Testing the sensor to higher and higher temperatures until failure to discover the true maximum temperature the HTIR-TC can withstand is another worthwhile course of study. Finally, the UT sensors desperately need development of data acquisition and processing software. Currently, the data is simply read from an oscilloscope and all post-processing must be done manually. This is mostly a hindrance in the efficient use of time and so inhibits the amount of testing with the sensor that can be effectively completed. This improvement is necessary to facilitated testing that will allow us to understand how the UT behaves under conditions like thermal transients and other dynamic processes.

Task V: Design of a Transient Reactor Test with Advanced Instrumentation:
We have developed white papers, theses and short research papers to describe our developments for use in the TREAT and other transient and steady state test programs. These have been uploaded to our PICS website for DOE use as appropriate.

COST STATUS: The IRP contract was delayed in it placement at UW-Madison by two months. In addition, the subcontracts to Idaho State, Kansas State and Ohio State were delayed until January 2015. Thus expenditures have lagged. As of the end of calendar year 2017 we have expended 96% of obligated funds. Final expenditures by our university team are being

SCHEDULE STATUS: There are no significant changes in the schedule (see below)

Task IA: Hodoscope Technology Enhancements
Task IA – 1: Collimator-based Hodoscope design, enhanced data-acquisition detector arrays
Task IA – 2: Cloud-chamber testing at ISU and based on results concept is not feasible
Task IA – 3: Modified Hornyak button concept that uses optical fibers for more light collection

Task	Q1	Q2	Q3	Q4	Q5	Q6	Q7	Q8	Q9	Q10	Q11	Q12
Task IA-1												
Task IA-2												
Task IA-3												
Quarterly, Annual, and Final Reports												

Task IB: High-Efficiency Neutron Detector Array
Task IB – 1: Design of the HENDA for use in the KSU TRIGA beamport
Task IB – 2: Fabricate HENDA and test with fuel pin motion in TRIGA
Task IB – 3: Efforts moved to MPFD work for out-of-pile and in-pile testing (Task IIA)

Task	Q1	Q2	Q3	Q4	Q5	Q6	Q7	Q8	Q9	Q10	Q11	Q12
Task IB-1												
Task IB-2												
Task IB-3												
Quarterly, Annual, and Final Reports												

Task IIA: Micro-pocket Fission Detectors
Task IIA – 1: High-temperature testing of MPFD at HTTL out-of-pile facility
Task IIA – 2: Optimize MPFD design for in-pile testing in KSU TRIGA reactor
Task IIA – 3: Continue to test MPFD in KSU TRIGA in collaboration with UW

Task	Q1	Q2	Q3	Q4	Q5	Q6	Q7	Q8	Q9	Q10	Q11	Q12
Task IIA-1												
Task IIA-2												
Task IIA-3												
Quarterly, Annual, and Final Reports												

Task IIB: Diamond Diode Temperature Sensor
Task IIB – 1: Fabrication & Characterization of diamond sensor for fuel rod application
Task IIB – 2: Out-of-Pile testing of diamond temperature sensor (revised thermistor design)
Task IIB – 3: In-pile testing of diamond temperature sensor in UW TRIGA reactor

Task	Q1	Q2	Q3	Q4	Q5	Q6	Q7	Q8	Q9	Q10	Q11	Q12
Task IIB-1												
Task IIB-2												
Task IIB-3												
Quarterly, Annual, and Final Reports												

Task IIC: Fiber Optic Temperature Sensors
Task IIC – 1: Fabrication and calibration of fiber optic sensor
Task IIC – 2: Out-of-Pile testing of fiber optic sensor
Task IIC – 3: In-pile testing of fiber optic sensor in UW TRIGA reactor

Task	Q1	Q2	Q3	Q4	Q5	Q6	Q7	Q8	Q9	Q10	Q11	Q12
Task IIC-1												
Task IIC-2												
Task IIC-3												
Quarterly, Annual, and Final Reports												

Task IID: HTIR-TC Fabrication for testing (Yr 1) and in-pile transient testing (Yr 2-3)

Task IIE: Ultrasonic Thermometer Fabrication, out-of-pile and in-pile transient testing

Task IIF: THWM-NP Fabrication for out of pile and in-pile transient testing

Task	Q1	Q2	Q3	Q4	Q5	Q6	Q7	Q8	Q9	Q10	Q11	Q12
Task IID:												
Task IIE:												
Task IIF:												
Quarterly, Annual, and Final Reports												

Task III and IV are covered in the testing program for the sensors as noted above:
Out-of-pile Testing: Task IA-2, Tasks IIB-2 and IIC-2, Task IID, Task II-E, Task IIF
In-pile Testing: Tasks IA-3 and IB-2, 3, Tasks IIA-3, IIB-3, IIC-3, II-D, II-E, II-F

Task V: Design of a Transient Reactor Test with Advanced Instrumentation: To begin in the first year of the project with input from our advisory committee group on testing needs. Design of the transient test will be accomplished at the end of the final year.

CHANGES IN SCOPE: There have been no changes in scope.

PROBLEMS ENCOUNTERED: There have been no major problems or delays encountered.

PERSONNEL and CHANGES: Prof. Jeremy Roberts has assumed Co-PI role at KSU.

ISU Personnel:	George Imel, PI; Students: Harishchandra Aryal; Cody Womak
KSU Personnel:	Jeremy Roberts, PI; D. McGregor, M.Harrison, Co-PIs Students: D. Nichols, R. Ghosh, W. Fu
OSU Personnel:	Tom Blue, PI, Students: B.Wilson, K. McCary, R. Palmer
UW Personnel:	M.Corradini, PI; M. Anderson, Co-PI, Paul Brooks, Students: J. Bredemann, T. Kim
INL Personnel:	Kurt Davis (PI), Josh Daw, Troy Unruh (D.Knudson – retired)

RESEARCH PRODUCTS:

Patents: 3 patent disclosure (KSU, OSU, UW)

Reviewed Publications:

Published/Accepted

A. Birri, Kelly McCary, Brandon Wilson, Thomas E. Blue, "Thermally Induced Bend Loss Analysis for Distributed Optical Sensing in Nuclear Reactors", Transactions of the American Nuclear Society 117 (2017)

John C. Boyington, Richard L. Reed, Ryan M. Ullrich, Jeremy A. Roberts. “Gamma-Ray and Thermal-Neutron Filter Design for a TRIGA Penetrating Beam Port.” Transactions of the American Nuclear Society, 117. 1162—1165 (2017)

J. Daw, et al., “Ultrasonic Transducer Irradiation Test Results,” 10th International Topical Meeting on Nuclear Plant Instrumentation, Control, and Human Machine Interface Technologies (NPIC&HMIT 2017), San Francisco, CA, June 11-15, 2017.

J. Daw, et al., “Update on Ultrasonic Thermometry Development at Idaho National Laboratory,” 10th International Topical Meeting on Nuclear Plant Instrumentation, Control, and Human Machine Interface Technologies (NPIC&HMIT 2017), San Francisco, CA, June 11-15, 2017.

M.J. Harrison, Michael A. Reichenberger, Daniel M. Nichols, Douglas S. McGregor, Jeremy A. Roberts. “Preliminary Analysis of Damage to MPFDs Caused by Reactor Pulses.” Transactions of the American Nuclear Society. 116. (2017)

P.Ghosh, Wenkai Fu, Ryan Fronk, Douglas S. McGregor, Jeremy A. Roberts. “Evaluation of MSNDs for Fast-Neutron Detection and the TREAT Hodoscope.” Transactions of the American Nuclear Society. 115. 109—112 (2016)

T.J.Kim, M.Anderson, Z.Ma, M.Corradini, “"High Temperature Diamond Thermistor for Nuclear Reactor”, Transactions of the American Nuclear Society 116 (2017)

D.M. Nichols, Michael A. Reichenberger, Sarah Stevenson, Tanner Swope, Caden Hilger, Jeremy A. Roberts, Nathaniel Edwards, Douglas S. McGregor. “Characterization of Argon, P-10, and Neon Ionization Gases for Use in Modular Micro-Pocket Fission Detector Arrays.” International Conference on Advancements in Nuclear Instrumentation Measurement Methods and their Applications, Liege, Belgium, June 19—23 (2017)

R.K. Palmer, Kelly M. McCary, Thomas E. Blue, "Time Constants for Optical Fiber Temperature Sensing using a Thermal Resistance Approach", Transactions of the American Nuclear Society 115 (2016).

R.K. Palmer, K. M. McCary and T. E. Blue, "An Analytical Model for the Time Constants of Optical Fiber Temperature Sensing," in IEEE Sensors Journal, vol. 17, no. 17, pp. 5492-5502, Sept.1, 1 2017.

R.K. Palmer, Kelly M. McCary, Thomas E. Blue, "Time Constants for Optical Fiber Temperature Sensing using a Thermal Resistance Approach", Transactions of the American Nuclear Society 115 (2016).

V.K. Patel, Michael A. Reichenberger, Jeremy A. Roberts, Troy C. Unruh, Douglas S. McGregor. “Simulated Performance of Micro-Pocket Fission Detectors (MPFDs) in the Transient REActor Test (TREAT) Facility using MCNP 6.” Annals of Nuclear Energy. 104. 191—196 (2017)

M.A. Reichenberger, Troy C. Unruh, Philip B. Ugorowski, Takashi Ito, Jeremy A. Roberts, Sarah R. Stevenson, Daniel M. Nichols, Douglas S. McGregor. “Micro-Pocket Fission Detectors (MPFDs) for In-Core Neutron Detection.” Annals of Nuclear Energy. 87. 318—323 (2016)

M.A. Reichenberger, Jeffrey A. Geuther, Daniel M. Nichols, Timothy J. Sobering, Jeremy A. Roberts, Philip B. Ugorowski, Douglas S. McGregor. “Electronic Support System Enhancements for Micro-Pocket Fission Detectors (MPFDs).” Proceedings of the IEEE Nuclear Science Symposium and Medical Imaging Conference, Seattle, WA, November 8—14 (2016)

M.A. Reichenberger, Daniel M. Nichols, Sarah Stevenson, Tanner Swope, Caden Hilger, Jeremy A. Roberts, Troy Unruh, Douglas S. McGregor. “Fabrication and Testing of a Modular MicroPocket Fission Detector Instrumentation System for Nuclear Test, Research, and Training Reactors.” International Conference on Advancements in Nuclear Instrumentation Measurement Methods and their Applications, Liege, Belgium, June 19—23 (2017)

J.A. Roberts, Mark Harrison, Wenkai Fu, Priyarshini Ghosh, Douglas S. McGregor, “Status of Fast-Neutron Detector Development at KSU for the TREAT Hodoscope.” In IRRMA 10. Chicago, IL, July 9—13 (2017)

B.A. Wilson, Tony Birri, Thomas E. Blue, "Evaluation of Optical Fiber Bragg Gratings in a Nuclear Reactor" Transactions of the American Nuclear Society 116 (2017)

B.A. Wilson, Kelly M. McCary, Thomas E. Blue, "Optimization of Silica Optical Fiber for High Temperature, Radiation Environments", Transactions of the American Nuclear Society 116 (2017)

To be Published/Submitted

A.Birri, Kelly McCary, Brandon Wilson, Thomas E. Blue, "Thermally Induced Bend Loss of Silica Optical Fiber", IEEE Sensors Journal, to be published

W. Fu, P. Ghosh, M.J. Harrison, D.S. McGregor, J.A. Roberts. “A Geant4 Evaluation of the Hornyak Button and Two Conceptual ZnS(Ag)-Based Detectors for the TREAT Hodoscope.” NIM A. to be published

W. Fu, P. Ghosh, M.J. Harrison, D.S. McGregor, J.A. Roberts. “Geant4 and MCNP6 Evaluations of Fast Sensitive Microstructured Semiconductor Neutron Detectors for the TREAT Hodoscope.” NIM A.

M.J. Harrison, D.S. McGregor, J.A. Roberts. “Radiation Hardness of Silicon Photomultipliers in Fast-Neutron Applications.” NIM A. to be published

T.J.Kim, K. Davis, M.Anderson, Z.Ma, M.Corradini, “"High Temperature Diamond Thermistor for Nuclear Reactor”, Review of Scientific Instruments, submitted 2017

R.S. Skifton, Palmer, A. J., Calderoni, P., “The Development of Calibration Procedures for High Temperature Irradiation Resistant Thermocouples,” Instrumentation Science and Technology, 2017 [accepted, in preparation]

B.A. Wilson and Thomas E. Blue, "Creation of an Internal Cladding in Sapphire Optical Fiber Enabling It to Produce Distributed Temperature Measurements by Optical Frequency Domain Reflectometry", IEEE Sensors Journal, to be published

B.A. Wilson, Thomas E. Blue, "Effect of Gamma-Ray and Neutron Heating as Interfering Input for the Measurement of Temperature Using Optical Fiber Sensor System", IEEE Sensors Journal, to be published

B.A. Wilson, Christian M. Petrie, Thomas E. Blue, " High Temperature Effects on the Light Transmission through Sapphire Optical Fiber", Journal of the American Ceramic Society, to be published

INL Report

Richard Skifton, Joe Palmer, Brian Jaques, Pattrick Calderoni and Troy Unruh., "Performance review of High Temperature Irradiation Resistant Thermocouples (HTIR-TC) in Out-of-pile and In-pile Tests," INL/INT-17-43511, September 2017.

Theses

J. Bredemann, "Advanced Temperature Sensors for Local Measurements during Transients in a Radiation Environment", M.S. Thesis, University of Wisconsin - Madison, December 2017

S. Mikael, "Carbon Material Growth, Characterization and Device Fabrication", Ph.D. Thesis, University of Wisconsin – Madison, January 2016

B. Wilson, "Evaluation of Optical Fiber Sensors in High Temperature and Nuclear Reactor Environments" Ph.D. Thesis, The Ohio State University, Columbus, OH, 2017

C.A. Womack, "The Construction and Characterization of a Large Volume Wilson Cloud Chamber Utilizing Orthogonal Cameras for Image Capture", M.S. Thesis, Idaho State University, December 2015

IRP Website: https://sites.google.com/a/wisc.edu/treat-restart-project/home